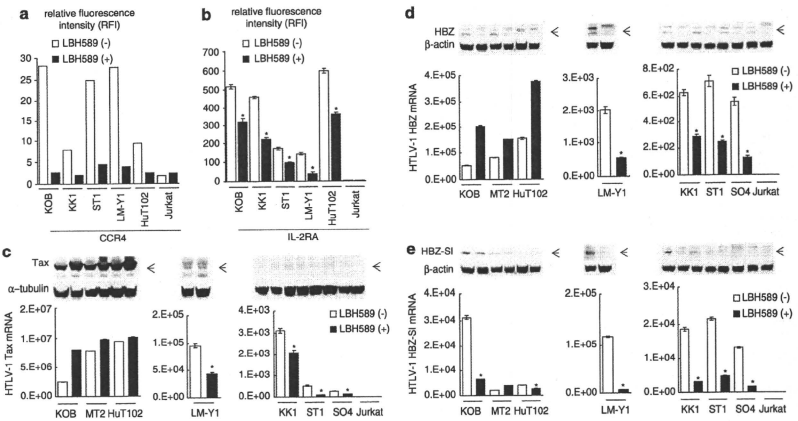

Figure 5 Effect of LBH589 on proteins characteristic of adult T-cell leukemia/lymphoma (ATLL) cells. Cells were treated with either vehicle or 50 nM of LBH589 for 24 h. After cells were harvested, flow cytometric analysis (FCM), real time quantitative RT-PCR and western blotting were performed. (**a** and **b**) Changes in expression of CCR4 and IL-2R were evaluated by FCM. The results were indicated using RFI. (**c**–**e**) Real-time quantitative RT-PCR and western blotting against HTLV-1 Tax, HBZ and HBZ-SI were performed as described in materials and methods. RT-PCRs were carried out in duplicate and the average value was used as the absolute amount of each mRNA. The cells were divided into three groups according to the amount of Tax mRNA; cell lines with high Tax mRNA levels (KOB, MT2 and HuT102), moderate levels (LM-Y1) and low levels (KK1 ST1 and SO4). The results of western blotting are also shown in each panel. (**b**–**e**) Results were expressed as the mean ± s.d. for three independent experiments and were also analyzed using Student's *t*-test. $^*P<0.01$.

expression of p53 in ST1 and KK1 as well as HuT102 cells without any accumulation of MDM2, which degrades p53 (Figure 6a). In contrast, the band of p21 was increased in intensity in these cell lines irrespective of their p53 status. Among apoptosis-related proteins downstream of p53, we found an increase in survivin, a decrease in XIAP, and no change in BAX, PUMA and Bcl-2 on treatment with LBH589 in ST1 or HuT102 cells. These results suggest that typical Bcl-2 family members are not involved in the permeabilization of the mitochondrial membrane in LBH589-induced apoptosis. Interestingly, LBH589 increased the expression of Bax and PUMA and decreased that of Bcl-2 and Bcl-xL in KK1 cells carrying a non-functional p53 mutation. These results indicate that LBH589 induced apoptosis in ATLL-related cell lines in a p53-independent manner.

Analysis of caspase-2-related apoptotic pathway

CASP2 and RIPK1 domain containing adaptor with death domain (also known as RAIDD), RIP, caspase-9 and cytochrome-*c* are involved in caspase-2-mediated apoptosis and were upregulated in their expression after LBH589 treatment (Table 1). The apoptosis induced by tumor necrosis factor-R1 requires the adaptor proteins TRADD, RIP and RAIDD in addition to caspase-2.[42] Recent reports suggest that caspase-2 can cause cytochrome-*c*'s release from mitochondria directly or indirectly.[43,44] Additionally, PIDD can interact with RAIDD and caspase-2, forming a PIDDosome and inducing apoptosis.[45] We investigated the expression profiles of caspase-2-related proteins by western blotting (Figures 6b and c). Caspase-2 was clearly activated by the treatment with LBH589 and cleaved forms were observed. Similar results were observed in TRAIL-treated Jurkat cells (Figure 6c). PIDD (90kDa) is constitutively processed into 51 and 37 kDa forms and cleaved PIDD (37 kDa) is essential for the activation of caspase-2.[46] Furthermore, upregulation of the expression of general forms of PIDD was observed during the activation of caspase-2 induced by genotoxic agents.[46] ATLL cell lines and Jurkat cells expressed various forms of PIDD, levels of which were not increased by LBH589 or TRAIL (Figures 6b and c). RIP was increased and TRADD was decreased in KK1 cells but neither was changed in ST1 or HuT102 cells. Of note, the activation of RAIDD was a common characteristic in these cells. Furthermore, the activation of RAIDD was also observed at the mRNA level in most of the ATLL-related cell lines (Figure 6d). In KK1 and ST1 cells, the activation of RAIDD mRNA expression was faint whereas that of protein production was obvious. We analyzed the 20s proteasome's activities to investigate whether RAIDD regulation by LBH589 in these cells is due to proteasome inhibition (Supplementary Figure 1C). Activities of 20S proteasome were dramatically impaired by MG132 in all cells examined and were not changed by LBH589 in KK1 and ST1 cells. The expression of RAIDD mRNA was not induced by the various chemicals used except LBH589 (Figure 6d, Supplementary Figure 1C, and data not shown). These results suggest that LBH589 caused the activation of caspase-2 and RAIDD without activating p53 and PIDD. We further observed the activation of RAIDD and caspase-2 in addition to acetylated histones in primary ATLL cells (Figure 6e).

LBH589 induces apoptosis in ATLL cells via caspase-2's activation

To further investigate the role of caspase-2-mediated apoptosis in LBH589-induced cell death, we first performed inhibition

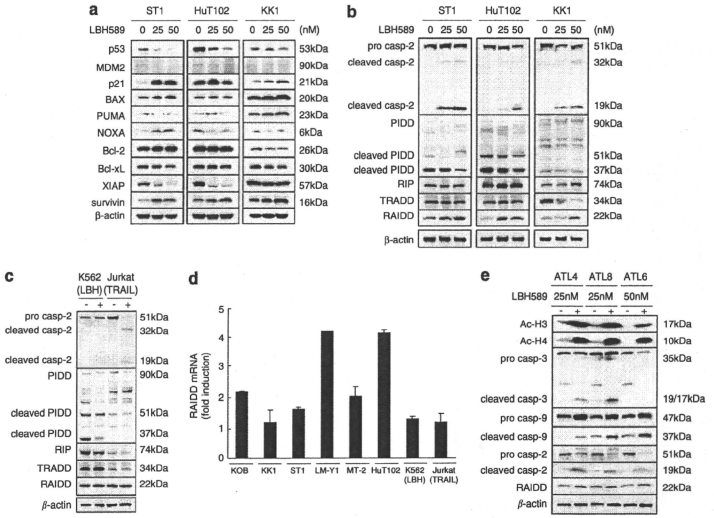

Figure 6 LBH589 activates RAIDD and caspase-2, but not p53. Whether the p53 pathway or caspase-2-related factors contribute to the LBH589-induced cell death was investigated by using ST1 and HuT102 (p53 wild type) cells, and KK1 (p53 mutated) cells. (**a**, **b** and **e**) Cells were treated with either vehicle or the indicated concentrations of LBH589 for 24 h. After cells were harvested, western blotting was performed. (**c**) Western blotting: tumor necrosis factor-related apoptosis-inducing ligand (TRAIL) (100 ng/ml)-treated Jurkat cells were used as a positive control of typical apoptosis and LBH589 (12 nM)-treated K562 cells were used as a negative control. (**d**) Activation of RAIDD by LBH589. After cells were treated with either vehicle or 50 nM of LBH589 for 24 h, real-time quantitative RT-PCR for RAIDD was performed. The fold increase in each cell line was obtained by setting the value for the expression without LBH589 as 1.0.

assays of caspases using specific inhibitors. The proportion of Annexin-V-positive cells among TRAIL-treated Jurkat cells was reduced from 67 to 20% by the pan-caspase inhibitor Z-VAD (Figure 7a). LBH589-induced cell death was also attenuated by Z-VAD with the percentage of Annexin-V-positive cells decreasing from 47 and 54% to 16 and 21% in ST1 and HuT102 cells, respectively. The caspase-8 inhibitor was not effective against LBH589-induced cell death, consistent with the finding that caspase-8 was not activated (Figure 4d). Importantly, the caspase-2 inhibitor Z-VDVAD had a similar effect to Z-VAD in LBH589-treated Jurkat cells, while it had a weak effect in TRAIL-treated cells (46%). Furthermore, western blotting revealed that the cleavage of caspase-3 by LBH589 was inhibited by Z-VDVAD as well as Z-VAD (not shown). These results suggest that LBH589 causes apoptosis in ATLL-related cell lines in a caspase-dependent manner and activation of caspase-2 is essential.

RAIDD as well as caspase-2 has a critical role in LBH589-induced apoptosis

Next, we performed siRNA experiments targeting caspase-2, caspase-9, RAIDD, PIDD and RIP to disclose the key triggers of apoptosis. Annexin-V/PI assays revealed that siRNA of RAIDD significantly repressed LBH-induced cell death, as did si-caspase-2 (Figure 7b). The proportion of Annexin-V-positive cells was ~65% in si-control cells and 37% in ST1 si-RAIDD cells. Similar results were obtained with HuT102 cells using siRNA set #1 (Figure 7b), set #2, and set #3 (Supplementary Figure 2C and E). Si-caspase-9 also inhibited LBH589-induced cell death while si-PIDD and si-RIP caused no change (Figure 7b). Similar inhibitory effects by si-RAIDD and si-caspase-2 were observed in JC-1 experiments (Figure 7c). The effect of si-caspase-9 was less extensive than that of si-PIDD or si-RIP (Figure 7c). These results suggest that RAIDD as well as caspase-2 has a critical role in LBH589-induced apoptosis and, importantly, they have active roles upstream of the mitochondria.

RAIDD has an initiating role in LBH589-induced apoptosis

Western blotting revealed that si-caspase-2 suppressed the cleavage of caspase-9, caspase-3 and PARP as well as the expression of caspase-2 itself. However, it could not suppress the activation of RAIDD (Figure 7d). Si-caspase-9 suppressed the cleavage of caspase-3 and PARP as well as the expression of caspase-9 itself, but could not suppress the activation of caspase-2 or RAIDD. Of note, si-RAIDD most effectively suppressed the cleavage of caspase-2, caspase-9, caspase-3 and PARP as well as the upregulation of RAIDD expression. Si-PIDD and si-RIP did not alter the expression profiles of caspases and RAIDD. These changes were basically similar in ST1 and HuT102 cells. An additional siRNA experiment was

performed using set #2 and set #3 siRNAs and results were similar to Figure 7d (Supplementary Figure 2D and F). The results indicate that the activation of RAIDD occurs upstream of the activation of caspase-2 and has an initiating role in LBH589-induced apoptosis.

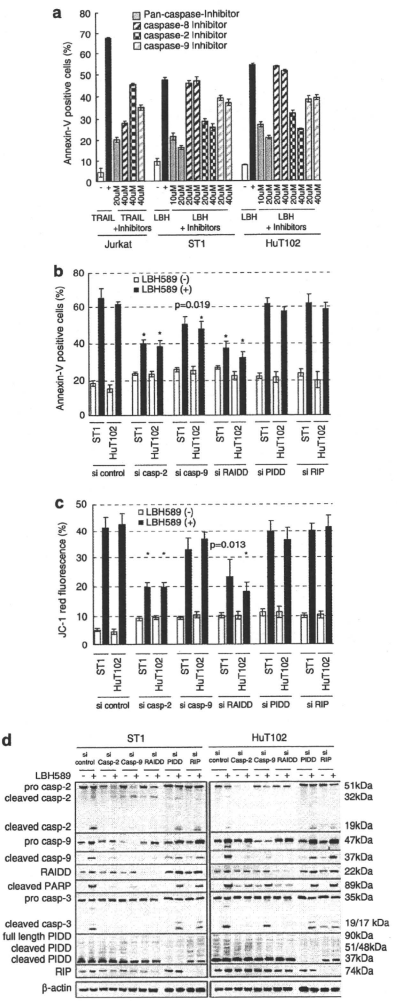

Discussion

DACi achieved significant biological effects in preclinical models of cancer including hematological malignancies which has led to clinical trials.[4,47–49] Then, it has become important to re-evaluate the mechanisms of tumor cell death caused by DACi. These processes will improve the design of further clinical trials and help in developing novel DACi. In this study, we showed that a newly developed DACi, LBH589, effectively induces ATLL cell death both *in vitro* and *in vivo* by a unique mechanism that has not been reported. Our findings uncovered a new role of caspase-2's activation in the induction of apoptosis.

It has been recognized that caspase-2-mediated apoptosis is initiated by death receptors.[42,50] However, recent studies revealed the ability of caspase-2 to engage the intrinsic pathway in response to DNA damage.[43,51–53] One possibility is that caspase-2 acts indirectly on the mitochondria, by cleaving the pro-apoptotic protein BID or by activating Bax and inducing the release of cytochrome-*C*.[44] Another alternative is that caspase-2 directly permeabilizes the mitochondrial membrane and stimulates the release of cytochrome-*C* independently of the Bcl-2 family including Bax and Bcl-2.[54] In addition, a recent report indicated that caspase-2 became activated in the so called PIDDosome, a complex of PIDD, caspase-2 and RAIDD, in a p53-dependent manner.[45] In our study, si-caspase-2 and si-RAIDD inhibited LBH589-induced apoptosis as well as permeabilization of the mitochondrial membrane. This mechanism is similar to the PIDDosome, however, LBH589-induced apoptosis was independent of p53 and PIDD was not activated. In addition, si-PIDD or si-RIP did not alter LBH589-induced apoptosis. Si-caspase-2 could not suppress the activation of RAIDD while si-RAIDD effectively suppressed the cleavage of caspase-2. These results indicated that LBH589 caused the activation of caspase-2 followed by RAIDD independent of p53 and PIDD. Regarding this point, a previous report suggested that caspase-2's activation occurred in a p53-independent manner.[55] Furthermore, two recent studies using PIDD-deficient mice demonstrated the PIDDosome-independent activation of caspase-2.[56,57] From our results, si-caspase-2 attenuated the LBH589-induced permeabilization of the mitochondrial membrane and the mRNA expression of cytochrome-*C* was highly upregulated by LBH589 probably due to cytochrome-*C*'s release. In contrast, most of the Bcl-2 family proteins were not altered by LBH589. In this regard, Robertson *et al.* suggested that caspase-2 can directly stimulate the intrinsic pathway independent of the Bcl-2 family.[43] More recently, Sidi *et al.*

Figure 7 RAIDD has a critical role in initiating LBH589-induced apoptosis. (**a**) Inhibition assay of caspases. Cells were treated with 25 nM of LBH589 or 100 ng/ml of tumor necrosis factor-related apoptosis-inducing ligand (TRAIL) with indicated concentrations of caspase-inhibitors for 24 h. Results were evaluated by Annexin-V/PI staining. Experiments were performed in triplicate and results were expressed as the mean ± s.d. (**b** and **c**) Effects of siRNA against caspase-2, caspase-9, RAIDD, PIDD and RIP. At 24 h after transfection, cells were incubated for 24 h with either vehicle or 50 nM of LBH589. Results were evaluated using Annexin-V/PI staining or the JC-1 dye and analyzed with flow cytometric analysis. Results were expressed as the mean ± s.d. for three independent experiments and were also analyzed using Student's *t*-test. $*P<0.01$ compared with si-control. (**d**) Western blotting. At 24 h after transfection, cells were incubated for 24 h with either vehicle or 50 nM of LBH589 and western blotting was performed.

demonstrated a caspase-2-dependent apoptotic program that bypasses a deficiency of p53 and excess of Bcl-2.[58] These reports are partly consistent with our own observations. However, our scenario does not work without the activation of RAIDD. Therefore, our results suggest that ATLL cells make use of a unique RAIDD-caspase-2-induced intrinsic pathway, which has not been reported previously. Additionally, as caspase-2-mediated apoptosis requires caspase-9,[51] upregulation of caspase-9 expression by LBH589 is advantageous to the induction of apoptosis. Although a number of independent studies strongly support a role for the intrinsic pathway in DACi-induced apoptosis, the mechanism remains to be fully elucidated.[1] Our findings may provide some explanation.

Although there is a consensus that the p53 pathway is inactivated by Tax in ATLL cells,[59] we recently found that ATLL-related cell lines expressing the wild-type p53 harbor an intact p53 pathway.[31] Some previous findings highlighted the importance of p53 in the effect of DACi, however, other studies demonstrated that the expression of wild-type p53 is not necessary for DACi-induced apoptosis.[2,60,61] Meanwhile, it has been reported that p21, downstream of p53, is activated by DACi independent of p53.[62,63] Indeed, the expression of p21 was increased by LBH589 in ATLL-related cell lines irrespective of their p53 status. In the present study, we clearly showed that LBH589 does not activate p53 in ATLL-related cell lines with the wild-type p53, and LBH589 was also effective against p53-mutant cells via the induction of a p53-like pro-apoptotic response. A similar phenomenon was reported previously in that the DACi FR901228 caused a p53-like pro-apoptotic response in p53 mutant cells and the degradation of the mutant p53 protein.[64] We further confirmed that LBH589 caused the degradation of p53 protein in p53 wild-type cells as well as p53-mutant cells. These results suggest that some types of DACi including LBH589 act upstream of the p53 pathway and cause the degradation of even mutated p53 protein via an unknown mechanism.

We also explored the ATLL-specific mechanisms in LBH589-induced cell death. Notably, CCR4 and IL-2R, well-known molecular targets in ATLL therapy, were repressed by the LBH589 treatment.[65,66] We speculated that Tax participates in the suppression of IL-2R, however, cells with high Tax mRNA levels actually showed an increase in Tax mRNA expression after LBH589 treatment. These results indicate that LBH589 can cause apoptosis even in Tax-expressing ATLL cells. In our study, mRNA levels of Tax and HBZ in ATLL-related cell lines were not inversely correlated. In addition, after treatment with LBH589, mRNA levels of Tax and HBZ changed in parallel. These results are not consistent with the idea that HBZ can inhibit Tax's activation.[19] Meanwhile, the expression of HBZ-SI was suppressed by LBH589 in most of the ATLL-related cell lines. Although the precise function of HBZ-SI is still under investigation,[24] a previous study found that inhibition of HBZ-SI by shRNA resulted in cell growth inhibition in ATLL cells.[23] Thus, HBZ-SI could potentially be a molecular target in ATLL therapy and the decrease in HBZ-SI caused by LBH589 treatment may also contribute to the apoptosis of ATLL cells. Consequently, we demonstrated that LBH589 is a promising drug against ATLL, and also identified a novel intrinsic pathway in LBH589-induced apoptosis.

Conflict of interest

The authors declare no conflict of interest.

Acknowledgements

We would like to express our gratitude to Dr Mesnard JM, Institut de Biologie, Laboratoire Centre d'étude d'agents Pathogènes et Biotechnologies pour la Santé Montpellier, France. Grant support note: This study was supported in part by a Grant-in-aid for Scientific Research (20590580) from the Japan Society for the Promotion of Science and a grant from Novartis.

References

1 Baylin SB, Ohm JE. Epigenetic gene silencing in cancer—a mechanism for early oncogenic pathway addiction? *Nat Rev Cancer* 2006; **2**: 107–116.
2 Bolden JE, Peart MJ, Johnstone RW. Anticancer activities of histone deacetylase inhibitors. *Nat Rev Drug Discov* 2006; **9**: 769–984.
3 Minucci S, Pelicci PG. Histone deacetylase inhibitors and the promise of epigenetic (and more) treatments for cancer. *Nat Rev Cancer* 2006; **1**: 38–51.
4 Xu WS, Parmigiani RB, Marks PA. Histone deacetylase inhibitors: molecular mechanisms of action. *Oncogene* 2007; **37**: 5541–5552.
5 Peart MJ, Tainton KM, Ruefli AA, Dear AE, Sedelies KA, O'Reilly LA *et al*. Novel mechanisms of apoptosis induced by histone deacetylase inhibitors. *Cancer Res* 2003; **63**: 4460–4471.
6 Henderson C, Mizzau M, Paroni G, Maestro R, Schneider C, Brancolini C. Role of caspases, Bid, and p53 in the apoptotic response triggered by histone deacetylase inhibitors trichostatin-A (TSA) and suberoylanilide hydroxamic acid (SAHA). *J Biol Chem* 2003; **14**: 12579–12589.
7 Mitsiades N, Mitsiades CS, Richardson PG, McMullan C, Poulaki V, Fanourakis G *et al*. Molecular sequelae of histone deacetylase inhibition in human malignant B cells. *Blood* 2003; **101**: 4055–4062.
8 Maiso P, Carvajal-Vergara X, Ocio EM, Lopez-Perez R, Mateo G, Gutierrez N *et al*. The histone deacetylase inhibitor LBH589 is a potent antimyeloma agent that overcomes drug resistance. *Cancer Res* 2006; **66**: 5781–5789.
9 Fulda S, Debatin KM. Extrinsic versus intrinsic apoptosis pathways in anticancer chemotherapy. *Oncogene* 2006; **25**: 4798–4811.
10 Bao Q, Shi Y. Apoptosome: a platform for the activation of initiator caspases. *Cell Death Differ* 2007; **14**: 56–65.
11 Nimmanapalli R, Fuino L, Bali P, Gasparetto M, Glozak M, Tao J *et al*. Histone deacetylase inhibitor LAQ824 both lowers expression and promotes proteasomal degradation of Bcr-Abl and induces apoptosis of imatinib mesylate-sensitive or -refractory chronic myelogenous leukemia-blast crisis cells. *Cancer Res* 2003; **63**: 5126–5135.
12 Bali P, Pranpat M, Bradner J, Balasis M, Fiskus W, Guo F *et al*. Inhibition of histone deacetylase 6 acetylates and disrupts the chaperone function of heat shock protein 90: a novel basis for antileukemia activity of histone deacetylase inhibitors. *J Biol Chem* 2005; **280**: 26729–26734.
13 Kovacs JJ, Murphy PJ, Gaillard S, Zhao X, Wu JT, Nicchitta CV *et al*. HDAC6 regulates Hsp90 acetylation and chaperone-dependent activation of glucocorticoid receptor. *Mol Cell* 2005; **18**: 601–607.
14 George P, Bali P, Annavarapu S, Scuto A, Fiskus W, Guo F *et al*. Combination of the histone deacetylase inhibitor LBH589 and the hsp90 inhibitor 17-AAG is highly active against human CML-BC cells and AML cells with activating mutation of FLT-3. *Blood* 2005; **105**: 1768–1776.
15 Fiskus W, Pranpat M, Bali P, Balasis M, Kumaraswamy S, Boyapalle S *et al*. Combined effects of novel tyrosine kinase inhibitor AMN107 and histone deacetylase inhibitor LBH589 against Bcr-Abl-expressing human leukemia cells. *Blood* 2006; **108**: 645–652.
16 Yamada Y, Tomonaga M. The current status of therapy for adult T-cell leukaemia-lymphoma in Japan. *Leuk Lymphoma* 2003; **44**: 611–618.
17 Yoshida M. Discovery of HTLV-1, the first human retrovirus, its unique regulatory mechanisms, and insights into pathogenesis. *Oncogene* 2005; **24**: 5931–5937.

18 Marriott SJ, Semmes OJ. Impact of HTLV-I Tax on cell cycle progression and the cellular DNA damage repair response. *Oncogene* 2005; **24**: 5986–5995.
19 Gaudray G, Gachon F, Basbous J, Biard-Piechaczyk M, Devaux C, Mesnard JM. The complementary strand of the human T-cell leukemia virus type 1 RNA genome encodes a bZIP transcription factor that down-regulates viral transcription. *J Virol* 2002; **76**: 12813–12822.
20 Arnold J, Yamamoto B, Li M, Phipps AJ, Younis I, Lairmore MD *et al*. Enhancement of infectivity and persistence *in vivo* by HBZ, a natural antisense coded protein of HTLV-1. *Blood* 2006; **107**: 3976–3982.
21 Cavanagh MH, Landry S, Audet B, Arpin-Andre C, Hivin P, Pare ME *et al*. HTLV-I antisense transcripts initiating in the 3'LTR are alternatively spliced and polyadenylated. *Retrovirology* 2006; **3**: 15.
22 Murata K, Hayashibara T, Sugahara K, Uemura A, Yamaguchi T, Harasawa H *et al*. A novel alternative splicing isoform of human T-cell leukemia virus type 1 bZIP factor (HBZ-SI) targets distinct subnuclear localization. *J Virol* 2006; **80**: 2495–2505.
23 Satou Y, Yasunaga J, Yoshida M, Matsuoka M. HTLV-I basic leucine zipper factor gene mRNA supports proliferation of adult T cell leukemia cells. *Proc Natl Acad Sci USA* 2006; **103**: 720–725.
24 Mesnard JM, Barbeau B, Devaux C. HBZ, a new important player in the mystery of adult T-cell leukemia. *Blood* 2006; **108**: 3979–3982.
25 Yamada Y, Tomonaga M, Fukuda H, Hanada S, Utsunomiya A, Tara M *et al*. A new G-CSF-supported combination chemotherapy, LSG15, for adult T-cell leukaemia-lymphoma: Japan Clinical Oncology Group Study 9303. *Br J Haematol* 2001; **113**: 375–382.
26 Tsukasaki K, Utsunomiya A, Fukuda H, Shibata T, Fukushima T, Takatsuka Y *et al*. VCAP-AMP-VECP compared with biweekly CHOP for adult T-cell leukemia-lymphoma: Japan Clinical Oncology Group Study JCOG9801. *J Clin Oncol* 2007; **25**: 5458–5464.
27 Maeda T, Yamada Y, Moriuchi R, Sugahara K, Tsuruda K, Joh T *et al*. Fas gene mutation in the progression of adult T cell leukemia. *J Exp Med* 1999; **189**: 1063–1071.
28 Hasegawa H, Yamada Y, Harasawa H, Tsuji T, Murata K, Sugahara K *et al*. Sensitivity of adult T-cell leukaemia lymphoma cells to tumour necrosis factor-related apoptosis-inducing ligand. *Br J Haematol* 2005; **128**: 253–265.
29 Yoshida M, Miyoshi I, Hinuma Y. Isolation and characterization of retrovirus from cell lines of human adult T-cell leukemia and its implication in the disease. *Proc Natl Acad Sci USA* 1982; **79**: 2031–2035.
30 Posner LE, Robert-Guroff M, Kalyanaraman VS, Poiesz BJ, Ruscetti FW, Fossieck B *et al*. Natural antibodies to the human T cell lymphoma virus in patients with cutaneous T cell lymphomas. *J Exp Med* 1981; **154**: 333–346.
31 Hasegawa H, Yamada Y, Iha H, Tsukasaki K, Nagai K, Atogami S *et al*. Activation of p53 by Nutlin-3a, an antagonist of MDM2, induces apoptosis and cellular senescence in adult T-cell leukemia cells. *Leukemia* 2009; **23**: 2090–2101.
32 Hasegawa H, Yamada Y, Komiyama K, Hayashi M, Ishibashi M, Sunazuka T *et al*. A novel natural compound, a cyclоanthranilylproline derivative (Fuligocandin B), sensitizes leukemia cells to apoptosis induced by tumor necrosis factor related apoptosis-inducing ligand (TRAIL) through 15-deoxy-Delta 12, 14 prostaglandin J2 production. *Blood* 2007; **110**: 1664–1674.
33 Usui T, Yanagihara K, Tsukasaki K, Murata K, Hasegawa H, Yamada Y *et al*. Characteristic expression of HTLV-1 basic zipper factor (HBZ) transcripts in HTLV-1 provirus-positive cells. *Retrovirology* 2008; **5**: 34.
34 Ramaswamy S, Nakamura N, Vazquez F, Batt DB, Perera S, Roberts TM *et al*. Regulation of G1 progression by the PTEN tumor suppressor protein is linked to inhibition of the phosphatidylinositol 3-kinase/Akt pathway. *Proc Natl Acad Sci USA* 1999; **96**: 2110–2115.
35 Fiskus W, Ren Y, Mohapatra A, Bali P, Mandawat A, Rao R *et al*. Hydroxamic acid analogue histone deacetylase inhibitors attenuate estrogen receptor-alpha levels and transcriptional activity: a result of hyperacetylation and inhibition of chaperone function of heat shock protein 90. *Clin Cancer Res* 2007; **13**: 4882–4890.
36 Cardone MH, Roy N, Stennicke HR, Salvesen GS, Franke TF, Stanbridge E *et al*. Regulation of cell death protease caspase-9 by phosphorylation. *Science* 1998; **282**: 1318–1321.
37 Yoshie O, Fujisawa R, Nakayama T, Harasawa H, Tago H, Izawa D *et al*. Frequent expression of CCR4 in adult T-cell leukemia and human T-cell leukemia virus type 1-transformed T cells. *Blood* 2002; **99**: 1505–1511.
38 Mori N, Fujii M, Ikeda S, Yamada Y, Tomonaga M, Ballard DW *et al*. Constitutive activation of NF-kappaB in primary adult T-cell leukemia cells. *Blood* 1999; **93**: 2360–2368.
39 Matsuoka M, Jeang KT. Human T-cell leukaemia virus type 1 (HTLV-1) infectivity and cellular transformation. *Nat Rev Cancer* 2007; **4**: 270–280.
40 Mori N, Matsuda T, Tadano M, Kinjo T, Yamada Y, Tsukasaki K *et al*. Apoptosis induced by the histone deacetylase inhibitor FR901228 in human T-cell leukemia virus type 1-infected T-cell lines and primary adult T-cell leukemia cells. *J Virol* 2004; **78**: 4582–4590.
41 Nishioka C, Ikezoe T, Yang J, Komatsu N, Bandobashi K, Taniguchi A *et al*. Histone deacetylase inhibitors induce growth arrest and apoptosis of HTLV-1-infected T-cells via blockade of signaling by nuclear factor kappaB. *Leuk Res* 2008; **32**: 287–296.
42 Duan H, Dixit VM. RAIDD is a new 'death' adaptor molecule. *Nature* 1997; **385**: 86–89.
43 Robertson JD, Enoksson M, Suomela M, Zhivotovsky B, Orrenius S. Caspase-2 acts upstream of mitochondria to promote cytochrome c release during etoposide-induced apoptosis. *J Biol Chem* 2002; **277**: 29803–29809.
44 Guo Y, Srinivasula SM, Druilhe A, Fernandes-Alnemri T, Alnemri ES. Caspase-2 induces apoptosis by releasing proapoptotic proteins from mitochondria. *J Biol Chem* 2002; **277**: 13430–13437.
45 Tinel A, Tschopp J. The PIDDosome, a protein complex implicated in activation of caspase-2 in response to genotoxic stress. *Science* 2004; **304**: 843–846.
46 Tinel A, Janssens S, Lippens S, Cuenin S, Logette E, Jaccard B *et al*. Autoproteolysis of PIDD marks the bifurcation between pro-death caspase-2 and pro-survival NF-kappaB pathway. *EMBO J* 2007; **26**: 197–208.
47 Rosato RR, Grant S. Histone deacetylase inhibitors in cancer therapy. *Cancer Biol Ther* 2003; **1**: 30–37.
48 Rasheed W, Bishton M, Johnstone RW, Prince HM. Histone deacetylase inhibitors in lymphoma and solid malignancies. *Expert Rev Anticancer Ther* 2008; **3**: 413–432.
49 Ellis L, Pan Y, Smyth GK, George DJ, McCormack C, Williams-Truax R *et al*. Histone deacetylase inhibitor panobinostat induces clinical responses with associated alterations in gene expression profiles in cutaneous T-cell lymphoma. *Clin Cancer Res* 2008; **14**: 4500–4510.
50 Ahmad M, Srinivasula SM, Wang L, Talanian RV, Litwack G, Fernandes-Alnemri T *et al*. CRADD, a novel human apoptotic adaptor molecule for caspase-2, and FasL/tumor necrosis factor receptor-interacting protein RIP. *Cancer Res* 1997; **57**: 615–619.
51 Lassus P, Opitz-Araya X, Lazebnik Y. Requirement for caspase-2 in stress-induced apoptosis before mitochondrial permeabilization. *Science* 2002; **297**: 1352–1354.
52 Zhivotovsky B, Orrenius S. Caspase-2 function in response to DNA damage. *Biochem Biophys Res Commun* 2005; **331**: 859–867.
53 Mhaidat NM, Wang Y, Kiejda KA, Zhang XD, Hersey P. Docetaxel-induced apoptosis in melanoma cells is dependent on activation of caspase-2. *Mol Cancer Ther* 2007; **6**: 752–761.
54 Robertson JD, Gogvadze V, Kropotov A, Vakifahmetoglu H, Zhivotovsky B, Orrenius S. Processed caspase-2 can induce mitochondria-mediated apoptosis independently of its enzymatic activity. *EMBO Rep* 2004; **6**: 643–648.
55 Castedo M, Perfettini JL, Roumier T, Valent A, Raslova H, Yakushijin K *et al*. Mitotic catastrophe constitutes a special case of apoptosis whose suppression entails aneuploidy. *Oncogene* 2004; **23**: 4362–4370.
56 Manzl C, Krumschnabel G, Bock F, Sohm B, Labi V, Baumgartner F *et al*. Caspase-2 activation in the absence of PIDDosome formation. *J Cell Biol* 2009; **185**: 291–303.
57 Kim IR, Murakami K, Chen NJ, Saibil SD, Matysiak-Zablocki E, Elford AR *et al*. DNA damage- and stress-induced apoptosis occurs independently of PIDD. *Apoptosis* 2009; **14**: 1039–1049.

58 Sidi S, Sanda T, Kennedy RD, Hagen AT, Jette CA, Hoffmans R *et al.* Chk1 suppresses a caspase-2 apoptotic response to DNA damage that bypasses p53, Bcl-2, and caspase-3. *Cell* 2008; **133**: 864–877.
59 Pise-Masison CA, Jeong SJ, Brady JN. Human T cell leukemia virus type 1: the role of Tax in leukemogenesis. *Arch Immunol Ther Exp (Warsz)* 2005; **53**: 283–296.
60 Ruefli AA, Ausserlechner MJ, Bernhard D, Sutton VR, Tainton KM, Kofler R *et al.* The histone deacetylase inhibitor and chemotherapeutic agent suberoylanilide hydroxamic acid (SAHA) induces a cell-death pathway characterized by cleavage of Bid and production of reactive oxygen species. *Proc Natl Acad Sci USA* 2001; **98**: 10833–10838.
61 Insinga A, Monestiroli S, Ronzoni S, Gelmetti V, Marchesi F, Viale A *et al.* Inhibitors of histone deacetylases induce tumor-selective apoptosis through activation of the death receptor pathway. *Nature Med* 2005; **11**: 71–76.
62 Richon VM, Sandhoff TW, Rifkind RA, Marks PA. Histone deacetylase inhibitor selectively induces p21WAF1 expression and gene-associated histone acetylation. *Proc Natl Acad Sci USA* 2000; **97**: 10014–10019.
63 Gui CY, Ngo L, Xu WS, Richon VM, Marks PA. Histone deacetylase (HDAC) inhibitor activation of p21WAF1 involves changes in promoter-associated proteins, including HDAC1. *Proc Natl Acad Sci USA* 2004; **101**: 1241–1246.
64 Blagosklonny MV, Trostel S, Kayastha G, Demidenko ZN, Vassilev LT, Romanova LY *et al.* Depletion of mutant p53 and cytotoxicity of histone deacetylase inhibitors. *Cancer Res* 2005; **65**: 7386–7392.
65 Ishida T, Ueda R. CCR4 as a novel molecular target for immunotherapy of cancer. *Cancer Sci* 2006; **11**: 1139–1146.
66 Chen J, Zhang M, Ju W, Waldmann TA. Effective treatment of a murine model of adult T-cell leukemia using depsipeptide and its combination with unmodified daclizumab directed toward CD25. *Blood* 2009; **113**: 1287–1293.

Supplementary Information accompanies the paper on the Leukemia website (http://www.nature.com/leu)

Published Ahead of Print on January 12, 2011, as doi:10.3324/haematol.2010.028605.

haematologica
the hematology journal

Early Release Paper

Overexpression of enhancer of zeste homolog 2 with trimethylation of lysine 27 on histone H3 in adult T-cell leukemia/lymphoma as a target for epigenetic therapy

by Daisuke Sasaki, Yoshitaka Imaizumi, Hiroo Hasegawa, Akemi Osaka, Kunihiro Tsukasaki, Young Lim Choi, Hiroyuki Mano, Victor Marquez, Tomayoshi Hayashi, Katsunori Yanagihara, Yuji Moriwaki, Yasushi Miyazaki, Shimeru Kamihira, and Yasuaki Yamada

Haematologica 2010 [Epub ahead of print]

Citation: Sasaki D, Imaizumi Y, Hasegawa H, Osaka A, Tsukasaki K, Choi YL, Mano H, Marquez V, Hayashi T, Yanagihara K, Moriwaki Y, Miyazaki Y, Kamihira S, and Yamada Y. Overexpression of enhancer of zeste homolog 2 with trimethylation of lysine 27 on histone H3 in adult T-cell leukemia/lymphoma as a target for epigenetic therapy. Haematologica. 2010; 95:xxx doi:10.3324/haematol.2010.028605

Haematologica (pISSN: 0390-6078, eISSN: 1592-8721, NLM ID: 0417435, www.haematologica.org) publishes peer-reviewed papers across all areas of experimental and clinical hematology. The journal is owned by the Ferrata Storti Foundation, a non-profit organization, and serves the scientific community with strict adherence to the principles of open access publishing (www.doaj.org). In addition, the journal makes every paper published immediately available in PubMed Central (PMC), the US National Institutes of Health (NIH) free digital archive of biomedical and life sciences journal literature.

Official Organ of the European Hematology Association
Published by the Ferrata Storti Foundation, Pavia, Italy
www.haematologica.org

DOI: 10.3324/haematol.2010.028605

Overexpression of enhancer of zeste homolog 2 with trimethylation of lysine 27 on histone H3 in adult T-cell leukemia/lymphoma as a target for epigenetic therapy

Daisuke Sasaki,[1] Yoshitaka Imaizumi,[2] Hiroo Hasegawa,[1] Akemi Osaka,[1] Kunihiro Tsukasaki,[2] Young Lim Choi,[3] Hiroyuki Mano,[3] Victor E. Marquez,[4] Tomayoshi Hayashi,[5] Katsunori Yanagihara,[1] Yuji Moriwaki,[2] Yasushi Miyazaki,[2] Shimeru Kamihira,[1] and Yasuaki Yamada[1]

[1]Department of Laboratory Medicine, Nagasaki University Graduate School of Biomedical Sciences, Nagasaki, Japan; [2]Department of Hematology and Molecular Medicine, Atomic Bomb Disease Institute, Nagasaki University Graduate School of Biomedical Sciences, Nagasaki, Japan; [3]Division of Functional Genomics, Jichi Medical University, Tochigi, Japan; [4]Chemical Biology Laboratory, National Cancer Institute, Frederick, MD, USA, and [5]Department of Pathology, Nagasaki University Hospital, Nagasaki, Japan

Funding

supported in part by a Grant-in-Aid for Scientific Research from the Ministry of Health, Labour, and Welfare of Japan (No. 04010119). For VEM, this research was supported in part by the Intramural Research Program of the NIH, Center for Cancer Research, NCI-Frederick.

DOI: 10.3324/haematol.2010.028605

Acknowledgments

The authors thank Sayaka Mori and Yuko Doi for excellent technical assistance.

Correspondence

Yasuaki Yamada, Department of Laboratory Medicine, 1-7-1 Sakamoto, Nagasaki 852-8501, Japan. Phone: international +81.2958197408.

Fax: international +81.959197422. E-mail: y-yamada@nagasaki-u.ac.jp

DOI: 10.3324/haematol.2010.028605

ABSTRACT

Background

Enhancer of zeste homolog 2 is a component of the Polycomb repressive complex 2 that mediates chromatin-based gene silencing through trimethylation of lysine 27 on histone H3. This complex plays vital roles in the regulation of development-specific gene expression.

Design and Methods

In this study, a comparative microarray analysis of gene expression in primary adult T-cell leukemia/lymphoma samples was performed, and the results were evaluated for their oncogenic and clinical significance.

Results

Significantly higher levels of *Enhancr of zeste homolog 2* and *RING1 and YY1 binding protein* transcripts with enhanced levels of trimethylation of lysine 27 on histone H3 were found in adult T-cell leukemia/lymphoma cells compared with those in normal CD4+ T-cells. Furthermore, there was an inverse correlation between the expression level of *Enhancer of zeste homolog 2* and that of miR-101 or miR-128a, suggesting that the altered expression of the latter miRNAs accounts for the overexpression of the former. Patients with high *Enhancer of zeste homolog 2* or *RING1 and YY1 binding protein* transcripts had a significantly worse prognosis than those without it, indicating a possible role

DOI: 10.3324/haematol.2010.028605

of these genes in the oncogenesis and progression of this disease. Indeed, adult T-cell leukemia/lymphoma cells were sensitive to a histone methylation inhibitor, 3-deazaneplanocin A. Furthermore, 3-deazaneplanocin A and histone deacetylase inhibitor panobinostat showed a synergistic effect in killing the cells.

Conclusions

These findings reveal that adult T-cell leukemia/lymphoma cells have deregulated Polycomb repressive complex 2 with overexpressed Enhancer of zeste homolog 2, and that there is the possibility of a new therapeutic strategy targeting histone methylation in this disease.

Introduction

The Polycomb group (PcG) proteins play critical roles in the regulation of development by repressing specific sets of developmental genes through chromatin modification.[1] They form two distinct multimeric complexes, Polycomb repressive complex 1 (PRC1) and PRC2, which bind to polycomb responsive elements (PRE), repress genes required for cell differentiation, and maintain pluripotency and self-renewal of embryonic stem cells and hematopoietic stem cells.[2,3] PRC2 consists of Enhancer of zeste homolog 2 (EZH2), which has histone methyltransferase activity, suppressor of zeste 12 (SUZ12), and embryonic ectoderm development (EED), which is required to maintain the integrity of PRC2.[1,4] Sequence-specific DNA binding protein YY1,

DOI: 10.3324/haematol.2010.028605

which recognizes PRE, interacts with EED and recruits PRC2 to a specific chromatin domain to be repressed.[5] EED interacts with histone deacetylase (HDAC) proteins, HDAC1 and HDAC2, and the histone binding proteins RBBP4 (RbAp48) and RBBP7 (RbAp46).[6] PRC2 thus also participates in histone deacetylation. EZH2, as a part of the PRC2 complex, not only methylates histone but also serves as a recruitment platform for DNA methyltransferases that methylate the promoter regions of target genes, which is another mechanism of gene repression.[7] The more diverse complex PRC1 consists of HPC family proteins that mediate chromatin association, HPH family proteins, RING, BMI1, and others.[1] PRC2 initiates trimethylation of lysine 27 on histone H3 (H3K27me3) and, to a lesser extent, lysine 9 of histone H3.[8] PRC1 recognizes H3K27me3 through the chromodomain of the HPC and maintains the trimethylation. There are a number of reports indicating that such epigenetically mediated transcriptional silencing is associated with cancer development.[1,9] Among these, oncogenic roles of overexpressed EZH2 have been studied in a variety of tumors.[10]

Adult T-cell leukemia/lymphoma (ATL) is a neoplasm of mature CD4+ T-cell origin, etiologically associated with human T-cell leukemia virus type-1 (HTLV-1).[11,12] Its clinical behavior is quite diverse among patients and is subclassified into four subtypes, smoldering type and chronic type as indolent subtypes, and acute type and lymphoma type as aggressive subtypes.[13] Inactivation of tumor suppressor genes is one of the key events in development and progression, and there is a strong accumulation of *p14ARF/p15INK4B/p16INK4A* gene deletion/methylation or *p53* gene mutations in aggressive subtypes (>60%).[14-20] In the present study, for further

DOI: 10.3324/haematol.2010.028605

investigation of the oncogenesis of ATL, we performed a comparative microarray analysis of gene expression in primary ATL samples. ATL cells expressed significantly higher levels of *EZH2* and *RYBP* (RING1 and YY1 binding protein) transcripts than CD4+ T cells from healthy volunteers. Moreover, acute-type ATL cells showed significantly higher levels of these transcripts than chronic-type ATL cells, suggesting that deregulation of PcG proteins plays a crucial role not only in the development but also in the progression of ATL. In addition, ATL samples were strongly positive for H3K27me3, and were sensitive to 3-deazaneplanocin A (DZNep), a histone methylation inhibitor.[21-23] It has recently been shown that HDAC inhibitor panobinostat (PS, also known as LBH589) depletes the levels of EZH2, SUZ12, and EED and induces apoptotic death in leukemia cells.[24] Deregulation of PcG protein genes with overexpressed EZH2 in ATL cells suggests that ATL is one of the appropriate target diseases for such epigenetic therapy.

Design and Methods

Sample preparation

This study was approved by the ethics committees of Nagasaki University, and all clinical samples were obtained after written informed consent was provided. The diagnosis of ATL was confirmed by the monoclonal integration of HTLV-1 proviral DNA in the genomic DNA of leukemia cells. Peripheral blood mononuclear cells (PBMCs) were obtained from ATL patients (acute type 22 cases, chronic type 19 cases) and healthy adult volunteers by density gradient

DOI: 10.3324/haematol.2010.028605

centrifugation using Lympho-prep (AXIS SHIELD, Oslo, Norway). For enrichment of ATL cells, CD4+ cells were purified from the PBMCs by the magnetic bead method (CD4 MicroBeads, Miltenyi Biotec, Auburn, CA) as described elsewhere.[25] Besides these samples for microarray analysis, we prepared another set of samples for quantitative real-time RT-PCR (qRT-PCR) and western blotting (25 ATL patients, 13 HTLV-1 carriers, and 12 healthy adults), to confirm the results of microarray analysis. We also used formalin-fixed, paraffin-embedded lymph nodes from 7 patients with lymphoma-type ATL and 5 patients with follicular lymphoma for immunohistochemical analysis.

ATL cell lines used in this study, SO4, ST1, KK1, KOB, and LM-Y1, were established from respective patients in our laboratory and have been confirmed to be of primary ATLL cell origin.[26] Cells were maintained in RPMI1640 medium supplemented with 10% FBS and 100 Japan reference units of recombinant interleukin-2 (rIL-2) (kindly provided by Takeda Pharmaceutical Company, Ltd., Osaka, Japan). We also used HTLV-1-infected T-cell lines MT2 and HuT102 and acute T-lymphoblastic leukemia cell lines Jurkat and MOLT4, which were maintained without rIL-2.

DNA microarray analysis

RNA was prepared from purified $CD4^+$ T cells, and subjected to hybridization to HGU133A & B microarray containing 44,760 probe sets for human genes (Affymetrix, Santa Clara, CA, USA) as described previously.[25,27] The mean expression intensity of the internal positive control probe sets (*http://www.affymetrix.com/support/technical/mask_files.affx*) was set to 500

DOI: 10.3324/haematol.2010.028605

units in each hybridization, and the fluorescence intensity of each test gene was normalized accordingly. All HGU133A & B microarray data are available at the Gene Expression Omnibus website (*http://www.ncbi.nlm.nih.gov/geo*) under the accession number GSE1466.

Quantitative real-time RT-PCR

For confirmation of the results of microarray analysis, we performed quantitative real-time RT-PCR (qRT-PCR) for PcG protein genes. Total RNA was prepared using Isogen (Wako, Osaka, Japan). After removal of contaminated DNA with DNase (Message Clean kit; GenHunter, Nashville, TN), cDNA was constructed from 1 μg of total RNA using the SuperScript III RT-PCR System (Invitrogen, Carlsbad, CA, USA) according to the manufacturer's instructions. Primers and TaqMan probes labeled with TAMRA dye at the 3' end and FAM at the 5' end are listed in Table 1. The mRNA levels for PcG family proteins and porphobilinogen deaminase (PBGD) were measured from a cDNA template using a LightCycler480 PCR System (Roche Diagnostics, Mannheim, Germany). Briefly, reactions were performed in a 20 μl volume with 5 μl (5 ng) of cDNA, 0.5 μM PCR primers, 0.1 μM TaqMan probes, and 10 μl of LightCycler 480 probes Master Mix (Roche Diagnostics). The PCR program consisted of 95°C for 5 min followed by 50 cycles of 95°C for 10 sec and 60°C for 30 sec. After 50 cycles, the absolute amounts of PcG protein mRNA and *PBGD* mRNA were interpolated from the standard curves generated by the dilution method using plasmids derived from a clone transfected with pTAC-1 Vector (BioDynamics Laboratory Inc., Tokyo, Japan) containing amplicons from the PcG family protein and *PBGD* genes, respectively. To normalize these results

DOI: 10.3324/haematol.2010.028605

for variability in concentration and integrity of RNA and cDNA, the *PBGD* gene was used as an internal control in each sample.

For the quantitative PCR for microRNAs (miRNAs), miR-101, miR-26a, and miR-128a, 10 ng of total RNA (containing miRNA) was used. RT reaction and real-time quantification were performed using TaqMan MicroRNA RT kit and TaqMan MicroRNA assays (hsa-miR-26a, assay ID 000405; hsa-miR-101, assay ID 002253; hsa-miR-128a, assay ID 002216; RNU6B, assay ID 001093) (Applied Biosystems, Foster City, CA, USA) in accordance with the manufacturer's instructions. Each PCR reaction mixture contained 10 μl of LightCycler 480 probes Master Mix, 4 μl of nuclease-free water, 1 μl of 20X specific PCR primer, and 5 μl of RT product. Thermal cycler was programmed as follows: 95°C for 5 minutes, 40 cycles of 95°C for 15 sec, and 60°C for 60 sec. Using the comparative CT method, we used an endogenous control (RNU6B) to normalize the expression levels of target micro-RNA by correcting differences in the amount of RNA loaded into qPCR reactions.

Western blot analysis and antibodies

Western blot analysis was performed as described previously.[28] The analysis was performed using antibodies to EZH2 and Histone H3 (Cell Signaling Technology, Danvers, MA, USA), phospho EZH2 (Ser21) (Bethyl Laboratories, Montgomery, TX), H3K27me3, dimethylated H3K27 (H3K27me2), monomethylated H3K27 (H3K27me1) (Millipore, Temecula, CA, USA), and β-actin (Sigma, St. Louis, MO, USA).

DOI: 10.3324/haematol.2010.028605

Immunohistochemistry

Immunohistochemical staining for EZH2 and H3K27me3 was performed on formalin-fixed, paraffin-embedded lymph node samples from lymphoma-type ATL patients and follicular lymphoma patients as a control. The deparaffinized slides were pretreated with DAKO Target Retrieval Solution, pH 9 (DAKO Japan, Tokyo, Japan), and heated in a water bath at 95°C for 40 minutes. For all stains, the endogenous peroxidase was quenched using 3% H_2O_2 for 15 minutes. Sections were then placed in 0.5% non-fat dry milk for 30 minutes at room temperature. The primary antibodies used were anti-EZH2 antibody (BD Biosciences, San Jose, CA, USA) and anti-H3K27me3 antibody (Cell Signaling Technology, Boston, MA, USA), and were applied at 1:50 dilution and 1:100 dilution, respectively. They were allowed to react for 1 hour at room temperature, and then the DAKO EnVision™ + Dual Link System-HRP (DAKO Japan, Tokyo, Japan) was applied using diaminobenzidine as the chromogen, following the manufacturer's protocol.

Sensitivity of adult T-cell leukemia/lymphoma cell lines to DZNep and PS (LBH589)

DZNep was synthesized by one of the authors, V.E.M. Cells were treated with different concentrations of DZNep for 72 hours and the cell proliferation status was evaluated by a MTS assay using a Cell Titer 96® AQueos Cell Proliferation Assay kit (Promega, Madison, WI, USA) in accordance with the manufacturer's instructions. To analyze the synergistic effect of combined treatment with DZNep and PS (LBH589) (kindly provided by Novartis Pharma AG, Basel, Switzerland), cells were treated with DZNep (0.3-5.0 μM) and PS

DOI: 10.3324/haematol.2010.028605

(LBH589) (3-50 nM) for 48 hours. After the cell proliferation status was evaluated by a MTS assay, the combination index (CI) for each drug combination was obtained by determining the median dose effect of Chou and Talalay using the CI equation within the commercially available software Calcusyn (Biosoft).[29] CI<1, CI=1, and CI>1 indicate synergism, additive effect, and antagonism, respectively. Cell viability represents the value relative to that of the control culture without these agents.

Results

Microarray analysis shows increased EZH2 and/or RYBP transcripts in adult T-cell leukemia/lymphoma cells

In a comparative microarray analysis of primary ATL samples, we focused on investigating PcG protein genes, *EZH2*, *RYBP*, *BMI-1,* and *CBX7,* in the present study because ATL cells show many aberrantly hypermethylated DNA sequences.[30] ATL cells expressed significantly higher levels of *EZH2* and *RYBP* transcripts than CD4+ T-cells from healthy adults (Figure 1A, B). In addition, there was a difference between ATL subtypes in these expressions, and cells from the acute type showed significantly higher levels of these transcripts than the cells from the chronic type. When patients were separated into two groups consisting of those with high expression and those with low expression, the group with high *EZH2* or high *RYBP* transcript showed significantly shorter survival than the respective low-expression groups (Figure 1E, F), indicating that high *EZH2* and/or *RYBP* expression is associated with

DOI: 10.3324/haematol.2010.028605

aggressive clinical behavior. Convincingly, there was a trend toward accumulation of acute-type ATL in high *EZH2* or high *RYBP* expression group: 14 cases of acute type and 6 cases of chronic type in high *EZH2* group, 7 cases of acute type and 13 cases of chronic type in low *EZH2* group, 14 cases of acute type and 6 cases of chronic type in high *RYBP* group, and 7 cases of acute type and 13 cases of chronic type in low *RYBP* group. BMI1 is known to downregulate the expression of *p14ARF/p16INK4A* and lead to neoplastic transformation.[31] Chromobox 7 (CBX7), a component of the PRC1, is also known to repress the transcription of *p14ARF/p16INK4A*.[32] Since inactivation of *p14ARF/p15INK4B/p16INK4A* genes is one of the key events in ATL progression, expression of *BMI-1* and/or *CBX7* transcript was expected to be elevated in acute-type ATL cells. There was however no difference in these expressions between ATL subtypes or even between ATL cells and normal CD4+ T-cells (Figure 1C, D). There was no difference in survival for different *BMI-1* or *CBX7* expression levels (Figure 1G, H).

Confirmation of increased EZH2 and/or RYBP transcripts by quantitative real-time RT-PCR

For confirmation of the results of microarray analysis, we quantified the transcripts of the PcG protein genes including *EZH2* and *RYBP* by qRT-PCR using another set of samples from ATL patients, healthy adults, HTLV-1 carriers, and hematologic cell lines including ATL cell lines. In accordance with the results of microarray analysis, *EZH2* and *RYBP* transcripts were increased in primary ATL cells compared with those in the cells from healthy adults and HTLV-1 carriers, with statistically significantly higher values in *EZH2* in terms of

DOI: 10.3324/haematol.2010.028605

both absolute copy number per 25 ng of total RNA and normalized expression level (Figure 2A, a, B, b). *RBBP4* was significantly higher in primary ATL cells than in the cells from healthy adults and HTLV-1 carriers in terms of normalized expression level (Figure 2C, c). In contrast, there was no difference in *BMI1*, *YY1*, and *EED* expressions among these groups, although some patients showed very high *BMI1* expression (Figure 2D, d, E, e, F, f). Similarly to primary ATL cells, some ATL cell lines showed high *EZH2* expression in terms of absolute copy number per 25 ng of total RNA (Figure 2A).

***EZH2* protein expression with trimethylation of H3K27 is characteristic in adult T-cell leukemia/lymphoma cells**

We then examined EZH2 and RYBP at the protein level by western blotting. A 98-kDa band for EZH2 protein and a 32-kDa band for RYBP protein were detected in all primary ATL samples irrespective of subtype, but they were hardly detected in cells from healthy adults and HTLV-1 carriers (Figure 3A, Supplementary Figure 1, and data not shown). ATL cell lines and acute T-lymphoblastic leukemia cell lines also showed intense EZH2 bands. The serine-threonine kinase Akt phosphorylates EZH2 at serine 21 and suppresses its methyltransferase activity by impeding EZH2 binding to histone H3, which results in a decrease in lysine 27 trimethylation.[33] EZH2 of ATL cells was not phosphorylated and was in its active form (Figure 3A). In fact, most primary ATL samples showed the band for H3K27me3, while the cells from healthy adults lacked the band (Figure 3B). As it is known that EZH2 plays a crucial role in trimethylation but not in dimethylation or monomethylation, the bands for H3K27me2 and H3K27me1 were detected in all samples examined, but the